Journal of Physics: Conference Series **1571** (2020) 012003 doi:10.1088/1742-6596/1571/1/012003

Active metamaterial polarization modulators for the Terahertz frequency range

Stephen J. Kindness[1], Nikita W. Almond[1], Wladislaw Michailow[1], Binbin Wei[1], Philipp Braeuninger-Weimer[2], Stephan Hofmann[2], Harvey E. Beere[1], David A. Ritchie[1] and Riccardo Degl'Innocenti[*, 3]

[1]Cavendish Laboratory, University of Cambridge, J. J. Thomson Avenue, Cambridge CB3 0HE, UK

[2]Department of Engineering, University of Cambridge, 9 J. J. Thomson Avenue, Cambridge CB3 0FA, UK

[3]Department of Engineering, University of Lancaster, Bailrigg, Lancaster LA1 4YW, UK.

*r.deglinnocenti@lancaster.ac.uk

Abstract. Active control of chirality in the terahertz frequency range is of great importance in many scientific areas, which include research into fundamental optical phenomena, investigation of novel materials, spectroscopy, imaging, wireless communications and chemistry. The lack of efficient, integrated and fast-reconfigurable polarization modulators has hindered, so far, the full exploitation of applications in all the aforementioned fields. Metamaterials are artificial resonant elements possessing unique remarkable properties such as high efficiency and miniaturization capability. The interplay of metallic metamaterial arrays with electrostatically tunable monolayer graphene has been demonstrated to be a valid approach for the realization of a novel class of THz devices. In this work, the realization of active chiral graphene/metamaterial modulator is presented. The versatility of this experimental approach allowed the device integration with broadband sources such as terahertz time domain spectrometers as well as with quantum cascade lasers. A continuous rotation of the polarization plane > 30° has been reported with a reconfiguration speed > 5 MHz. These results pave the way to the integration of fast terahertz polarization modulators in all the applications where these devices are in great demand.

1. Introduction

Integrated, all-electronic terahertz (THz) modulators [1] are of utmost importance in the myriad of applications where active control of this radiation is required, e.g. for the next generation of wireless communications, investigation of novel materials, such as topological insulators, spectroscopy and imaging. The achievement of an efficient manipulation of THz radiation has proved to be particularly elusive because of the lack of efficient and fast-reconfigurable modulators. Metamaterials [2, 3], subwavelength elements engineered to yield an artificial electromagnetic response, are the best candidates to overcome the poor properties exhibited by the naturally occurring materials in this frequency range. THz active optoelectronic devices based on metamaterials have been successfully demonstrated [4, 5]. Among these, chiral metamaterial-based polarization modulators [6, 7] have

attracted a great attention due to the unique importance of THz polarization control for chemistry, biology, and spectroscopic applications. In this work we present a chiral modulator architecture based on a metallic metasurface for the control of optical activity and circular dichroism. The devices were efficiently integrated with a terahertz time domain spectroscopic (THz-TDS) system and a powerful, narrow linewidth quantum cascade laser (QCL).

2. Design and Fabrication

The metamaterial unit in the device was based on the coupling between a bright resonator and two dark resonators as showed in figure 1 a). The fundamental unit cell was replicated into a 1.7 mm^2 metamaterial array for efficient light coupling. The device was fabricated using standard optical and electron beam lithography followed by a Ti/Au (10/100 nm) thermal metallic evaporation to define the

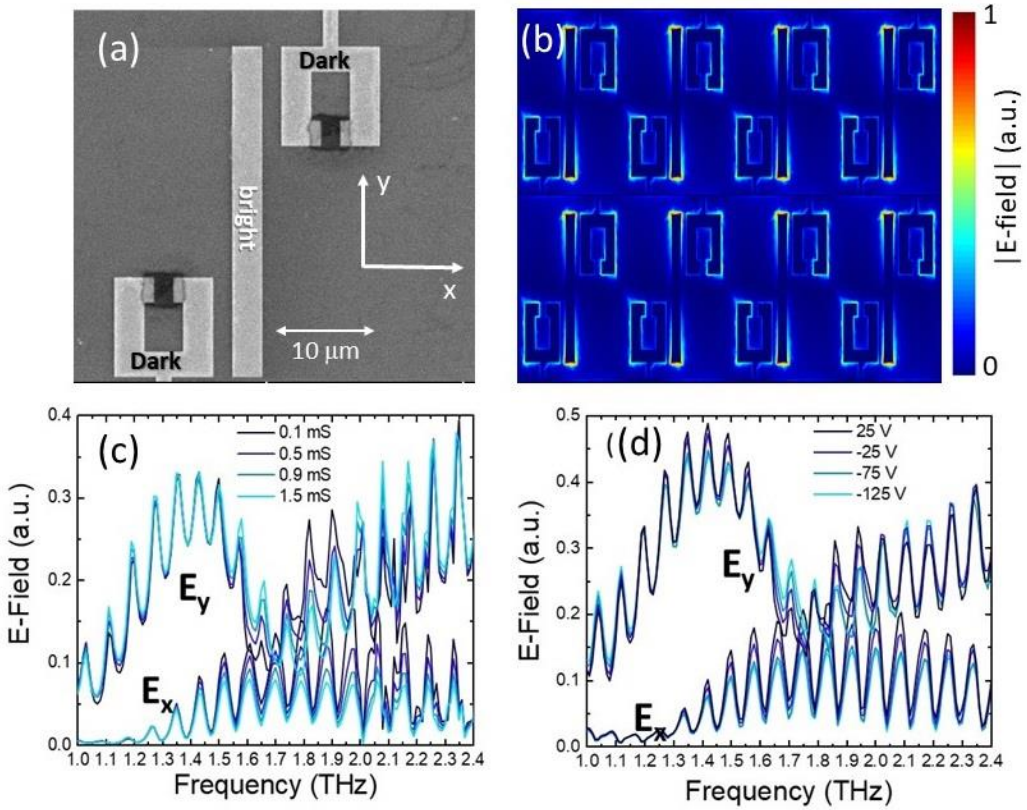

Figure 1. Scanning electron picture of a chiral unit cell (a); it is possible to distinguish the two graphene areas shunting the gaps in the dark resonators. Sketch of the array with the |E-field| norm at resonance (b). Numerical simulations of the $E_{x,y}$ transmitted components and measured values, (c) and (d) respectively, for different graphene conductivities/back gate voltages.

array and the bonding pads on a SiO_2/Si (300 nm/500 µm) chip. The Si substrate was p-doped to allow electrostatic backgating of the sample. Monolayer graphene grown via chemical vapor deposition was transferred on top of the gold resonator arrays and then patterned into patches shunting the dark resonators. The dark resonators were variably damped by changing the graphene's conductivity, hence electrically acting on the coupling condition and modulating the transmitted polarization angle, as detailed in Ref. [6]. The orientation of these resonators is such that a radiating electric dipole orthogonal (E_x) to the incident electric field (E_y) polarization is induced, causing a rotation of the polarization angle of the transmitted radiation.

3. Numerical simulations and experimental results

The single unit cell was investigated with the help of the finite element software Comsol Multiphysics, v5.3a; further details on the numerical simulations are reported in Ref. [6]. The calculated absolute value

of the electric field (|E-field|) mode distribution in the array is shown in figure 1 (b). The numerical results obtained for the transmitted E-field components E_x, and E_y, are presented in figure 1 (c) for different conductivity values. A broad resonance corresponding to a dip in the E_y component and a peak in the E_x component is observed at ~1.7 THz. The polarization modulator was characterized with a fiber-coupled THz time domain spectrometer set-up from Menlo systems, model Tera K15, modified to extract the transmitted electric field polarization components for different backgate voltages. The experimental results are presented in figure 1 (d) and show an excellent agreement with the numerical simulations of figure 1 (c). The graphene charge neutrality point was experimentally found at ~ +25 V. The back voltage range between -125 V and +25 V corresponded to a graphene conductivity range from 1.3 mS to 0.3 mS, respectively. Clear Fabry-Perot resonances, due to the reflections at the device boundaries, are observed in figure 1 (c) and (d). The effect of these resonances need to be considered when integrating the modulator device with narrow linewidth sources, such as QCLs. The polar plots showed in figure 2 were calculated from the acquired E_x, E_y waveforms. A maximal continuous rotation of ~32° at 1.73 THz was measured for the polarization plane, with an ellipticity of 0.4, as defined in Ref. [6]. The corresponding polar plot is shown in figure 2 (a). Figure 2 (b) instead, calculated at 1.75 THz, presented a reduced ellipticity and a rotation angle of ~20°. Interestingly in figure 2 (b) the ellipticity handedness changed from -0.15 to 0.15 when sweeping the voltage range. Finally, figure 2 (c) shows a modulation of the ellipticity of 0.5 with a minimal change of the polarization plane: an

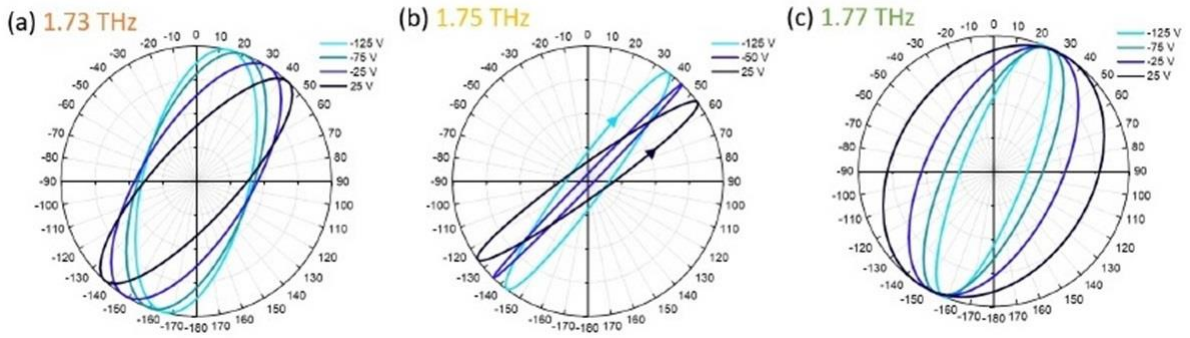

Figure 2. Polar plots calculated from the experimental acquired waveforms at 1.73 THz (a), 1.75 THz (b), and 1.77 THz (c).

almost pure circular dichroism without optical activity. The chiral modulator was finally integrated in a cross-polarized apparatus having a QCL emitting at 1.9 THz as the source. In this configuration the device was operating as an amplitude modulator with a reconfiguration speed > 5 MHz. In conclusion, in this work a chiral modulator based on the interplay between graphene and a metamaterial array was presented. Depending of the experimental configuration, the features of the device consisted in the achievement of tunable optical activity, circular dichroism and, amplitude modulation with different THz sources. The high efficiency and versatility of this approach would help unlocking a myriad of applications in the THz range.

References

[1] Degl'Innocenti R, Kindness S J, Beere H E, Ritchie D A 2018 *Nanophotonics* **7**(1) 127–144.
[2] Chen H T, Taylor A J, Yu N 2016 *Rep. Prog. Phys.* **79** 076401.
[3] Lee S, Baek S, Kim T-T, Cho H, Lee S, Kang J-H, Min B 2020 *Adv. Mater.* 2000250.
[4] Kindness S J, Almond N W, Wei B, Wallis R, Michailow W, Kamboj V S, Braeuninger-Weimer P, Hofmann S, Beere H E, Ritchie D A, Degl'Innocenti R 2018 *Adv. Optical Mater*. **6** 1800570.
[5] Kindness S J, Jessop D S, Wei B, Wallis R, Kamboj V S, Xiao L, Ren Y, Braeuninger-Weimer P, Aria A I, Hofmann S, Beere H E, Ritchie D A, Degl'Innocenti R 2017 *Sci. Rep*. **7** 1.
[6] Kindness S J, Almond N W, Michailow W, Wei B, Jakob L A, Delfanazari K, Braeuninger-Weimer P, Hofmann S, Beere H E, Ritchie D A, Degl'Innocenti R 2019 *ACS Photonics* **6**

1547.
[7] Oh S S, Hess O 2015 *Nano Convergence* **2** 24.

Acknowledgments

S.J.K. acknowledges the Integrated Photonic and Electronic Systems CDT (Grant No. EP/L015455/1) for funding and support. S.J.K., N.W.A., B.W., W.M., H.E.B., D.A.R. acknowledge financial support from the Engineering and Physical Sciences Research Council (EPSRC) (Grant No. EP/P021859/1, Hyper Terahertz). W.M. thanks the George and Lillian Schiff Foundation of the University of Cambridge for financial support and is grateful for the Honorary Vice-Chancellor's Award of the Cambridge Trust. R.D. acknowledges support from the EPSRC (Grant No EP/S019383/1) and from the Royal Society (RSG/R1/180148 – Research Grant). S.H. and P.B.W. acknowledge funding from the EPSRC (Grant No. EP/K016636/1). P.B.W. acknowledges the EPSRC Cambridge NanoDTC (Grant No. EP/G037221/1).